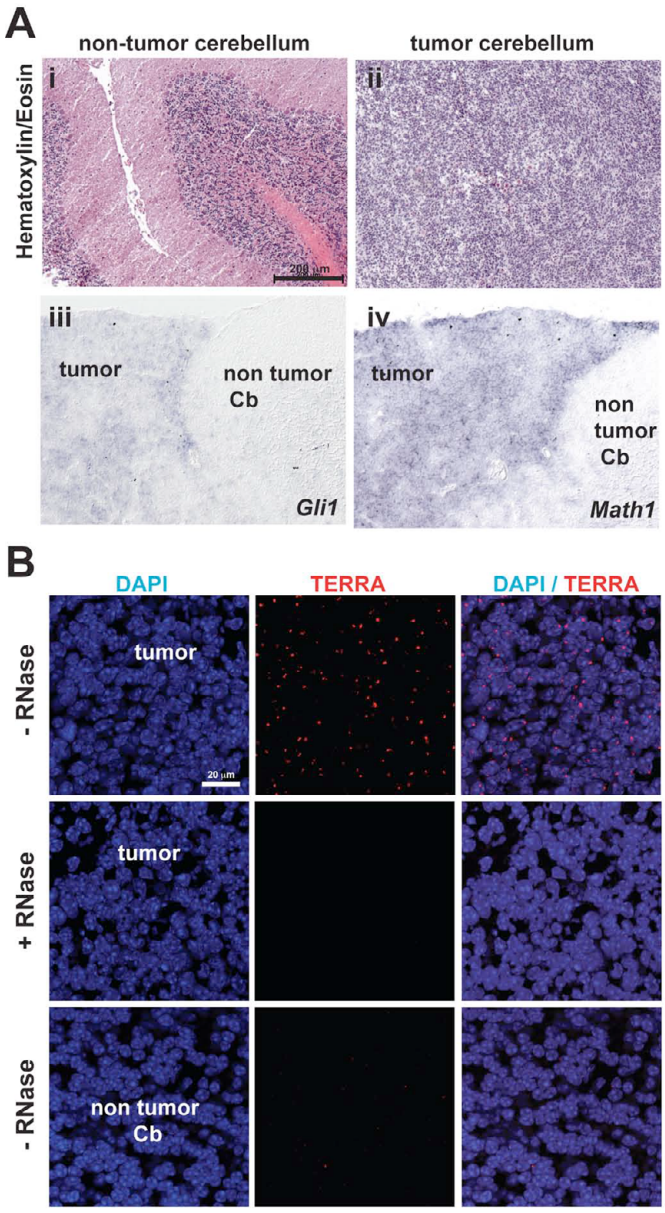

Fig. S1. TERRA is highly expressed in primary medulloblastoma. (A) Upper panels: Hematoxylin/Eosin staining of a region of a *Ptch1*$^{+/-}$ mouse cerebellum with non-tumor and tumor tissue (#7040). The normal morphology of cerebellar folia with the IGL (containing the mature granule neurons) and the Purkinje layer containing the Purkinje neurons is seen in non-tumor cerebellum. Scale bar=200 µm. Lower panels: sections of cerebellum containing both non-tumor and tumor tissue showing the results of in situ hybridizations with specific digoxigenin-labeled RNA probes for *Gli1* and *Math1*. Note that *Gli1* and *Math1* are highly expressed in the tumor part of the cerebellum. (B) Confocal images of FISH analyses for TERRA expression in sections of the cerebellum of the same mouse as above containing both non-tumor and tumor tissue. Note the presence of TERRA expression (strong red labeling) in the tumor as compared to the undetectable expression in the non-tumor cerebellar tissue. RNase A treatment leads to an elimination of the tumor specific TERRA signal. Scale bar=20 µm.

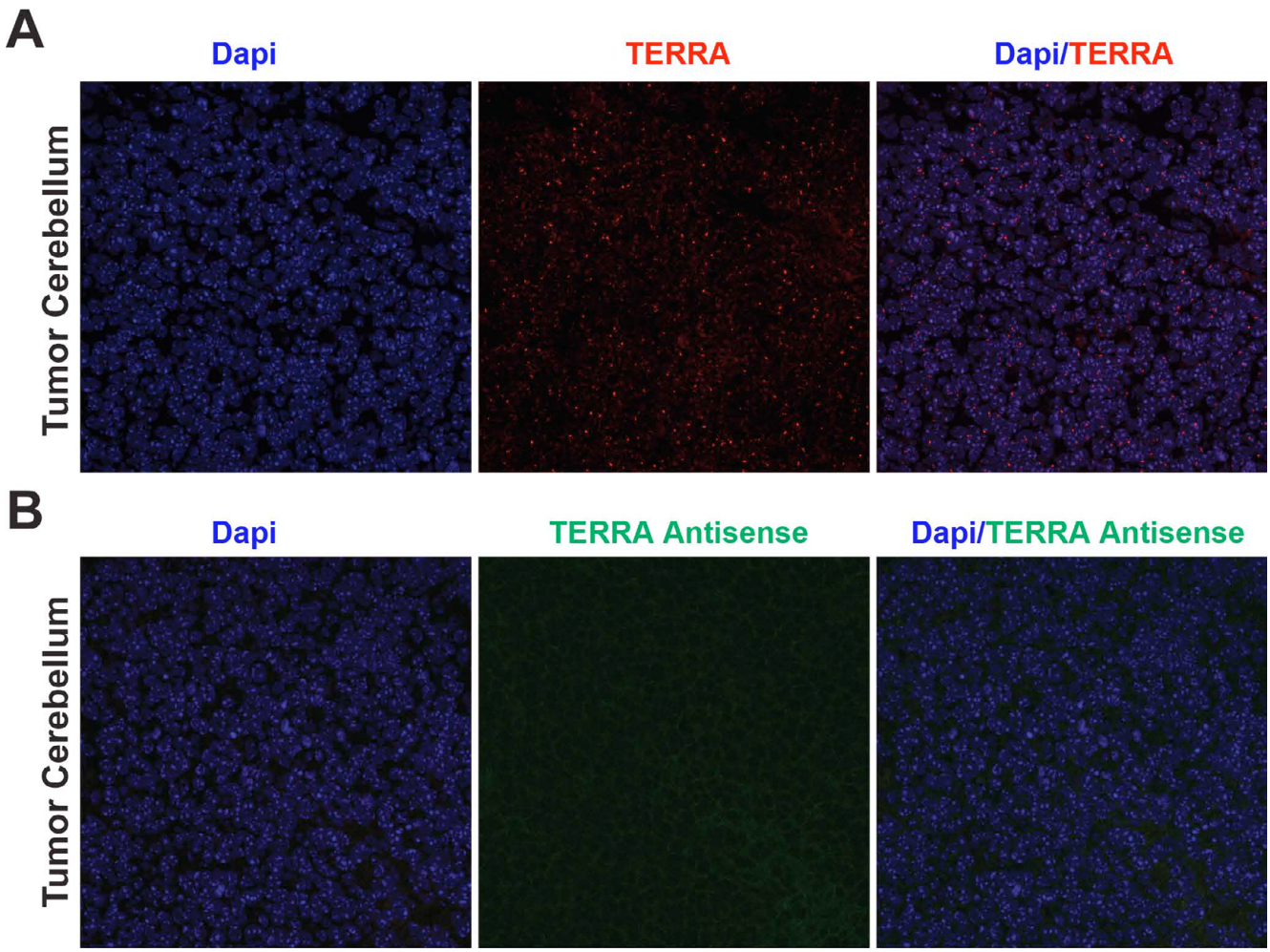

Fig. S2. TERRA antisense is not detected in mouse medulloblastoma. Confocal images of FISH analyses for TERRA and TERRA antisense expression in sections of the cerebellum of the same mouse as above containing both non-tumor and tumor tissue. TERRA antisense was detected by a FAM-conjugated $(TTAGGG)_3$ PNA probe, while TERRA was detected by a TAMRA-conjugated $(CCCTAA)_3$ PNA probe. Images were taken with 40× lens with 2× zoom.

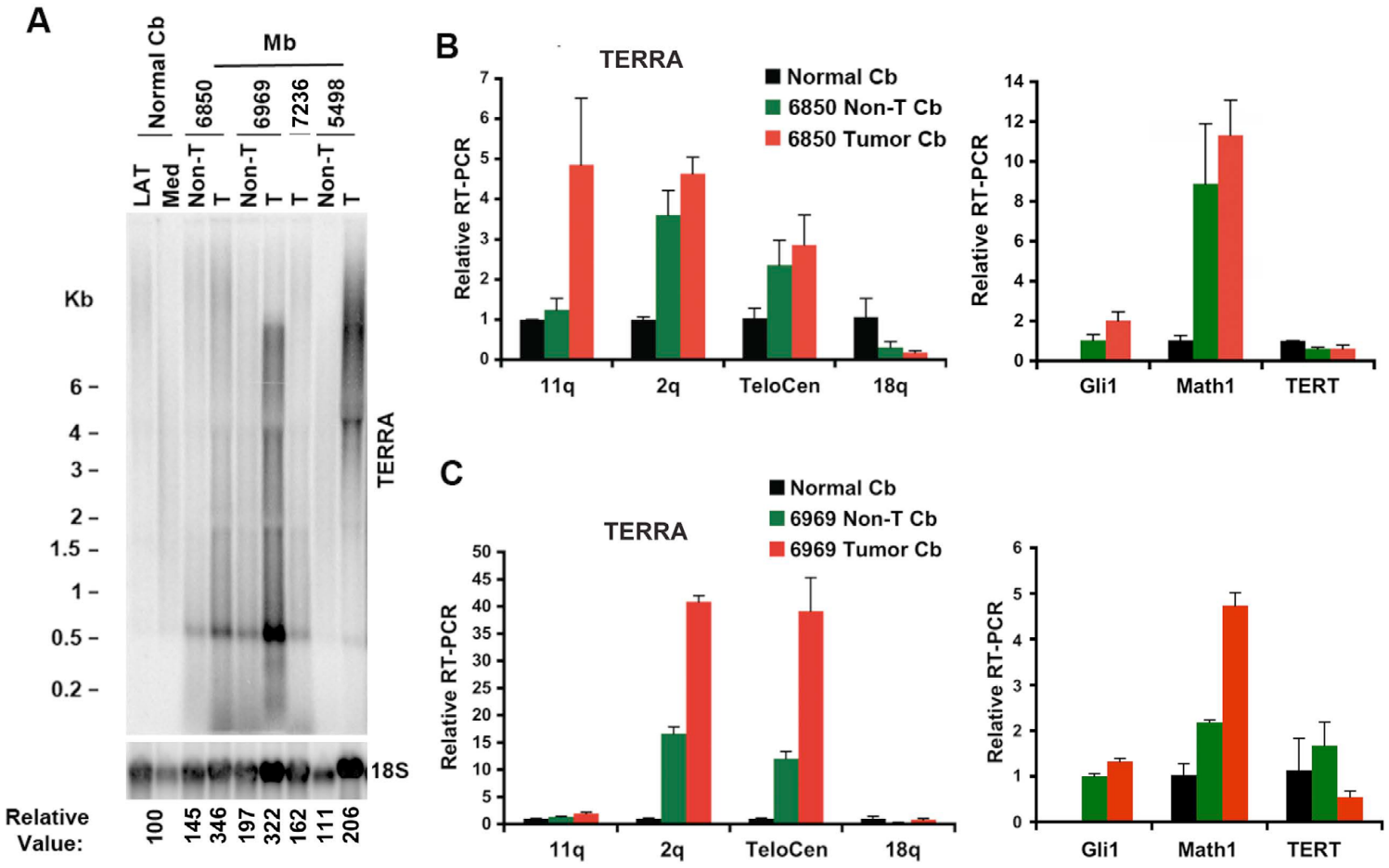

Fig. S3. Primary mouse medulloblastoma express high levels of TERRA RNA. (A) Total RNA was assayed by Northern blot and the blot was first probed with ^{32}P-labeled $(TAACCC)_4$ for TERRA RNA expression. 18S RNA expression is shown as quantification control. Numbers on the left show the position of markers in kb. Normal cerebellum was dissected [both the medial (Med) and lateral part (LAT)] as well as three different mouse medulloblastoma (both non-tumor and tumor part) were assessed for TERRA expression. Quantification of TERRA levels detected in this Northern blot (relative to 18S level) show a moderate increase of TERRA expression in pre-cancerous tissues (non-tumor part of a *Ptch1*$^{+/-}$ background cerebellum developing a medulloblastoma) and a large increase in the tumor part as compared to the normal cerebellum. (B) Quantitative RT-PCR analysis of expression of *Math1*, *Gli1,* and *Tert* in non-tumor and tumor cerebellum in medulloblastoma #6850 (Right panel). TERRA RNA was examined in non-tumor and tumor cerebellum in medulloblastoma #6850 using primers specific for TERRA RNA transcribed from subtelomeres of chromosome 2q, 11q, 18q, and telocentric chromosomes (Telocen) (Left panel). Relative RT-PCR represents the value calculated by ΔΔCT methods relative to normal cerebellum (LAT) and *Gapdh*, except *Gli1* where ΔΔCT methods relative to Non-T Cb and *Gapdh* were used due to no detectable levels of *Gli1* expression in normal cerebellum (LAT). Bar graph represents the average value from three independent PCR reactions (mean ± s.d.). (C) Quantitative RT-PCR analysis of expression of *Math1, Gli1,* and *Tert* in non-tumor and tumor cerebellum in medulloblastoma #6969 (Right panel). TERRA RNA was examined using primers specific for TERRA RNA transcribed from subtelomeres of chromosome 2q, 11q, 18q, and telocentric chromosomes (Telocen) (Left panel). Relative RT-PCR represents the value calculated by ΔΔCT methods relative to normal cerebellum (LAT) and *Gapdh*. Bar graph represents the average value from three independent PCR reactions (mean ± s.d.). For both tumor tested, note the increase in individual TERRA RNA expression from chr 2q, 11q and telocen.

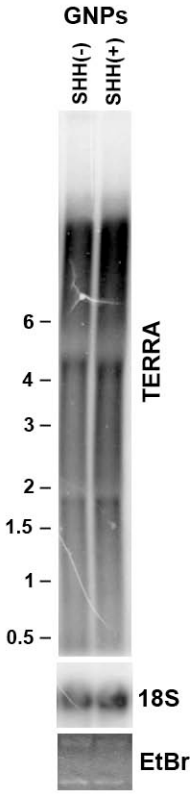

Fig. S4. Another example of TERRA induction in purified progenitor cells stimulated with SHH in vitro. GNPs were purified from wild-type mouse P5 cerebella and cultured for 12 hours with or without SHH (600 ng/ml). TERRA RNA was analyzed by northern blot using ^{32}P-labelled $(TAACCC)_4$ oligonucleotide probe. 18S RNA expression is shown as internal control for RNA loading. EtBr staining shows the integrity of RNA used in the assay.

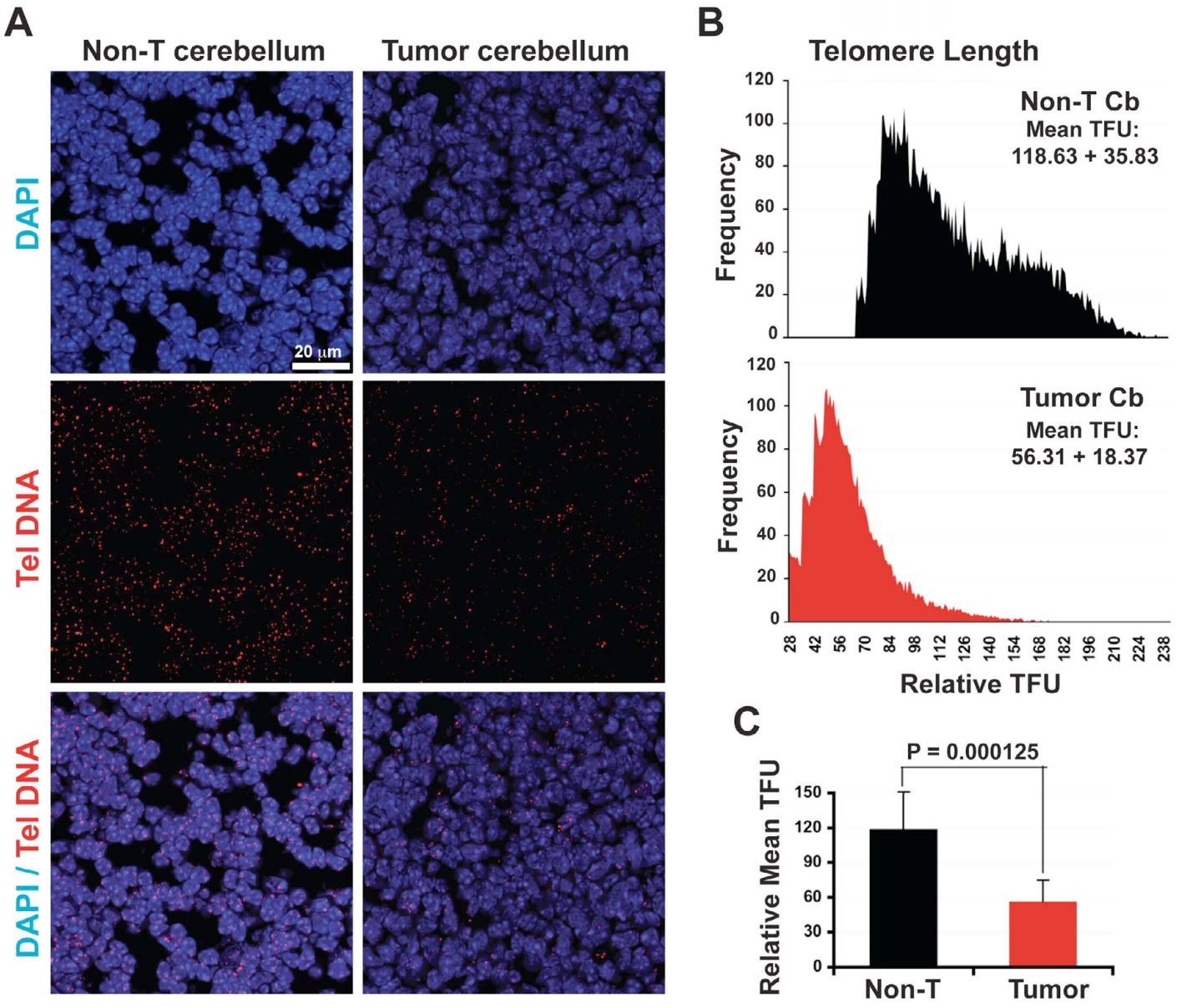

Fig. S5. Telomere DNA FISH of mouse normal and medulloblastoma tumor tissue. (A) Representative Confocal image for telomere DNA FISH on cerebellum section containing both non-tumor and a tumor parts (same tumor as in Fig. 1). Note the reduced telomeric DNA signal (Red) in the tumor when compared to the non-tumor part of the cancerous cerebellum. All nuclei are counterstained with DAPI (blue). Scale bar=20 μm. (B) Histogram comparing average telomere length in Non-tumor (black) verse Tumor (red). Telomere length is measured by relative telomere DNA FISH fluorescence unit (TFU) as a function of frequency of occurrence. (C) Telomere length comparison using total mean fluorescence intensity of telomere DNA FISH foci in non-tumor (black) vs tumor (red). Standard deviations were derived from quantification of more than 800 nuclei from at least three independent experiments. *P*-value was calculated by two-tailed Student's t-test.

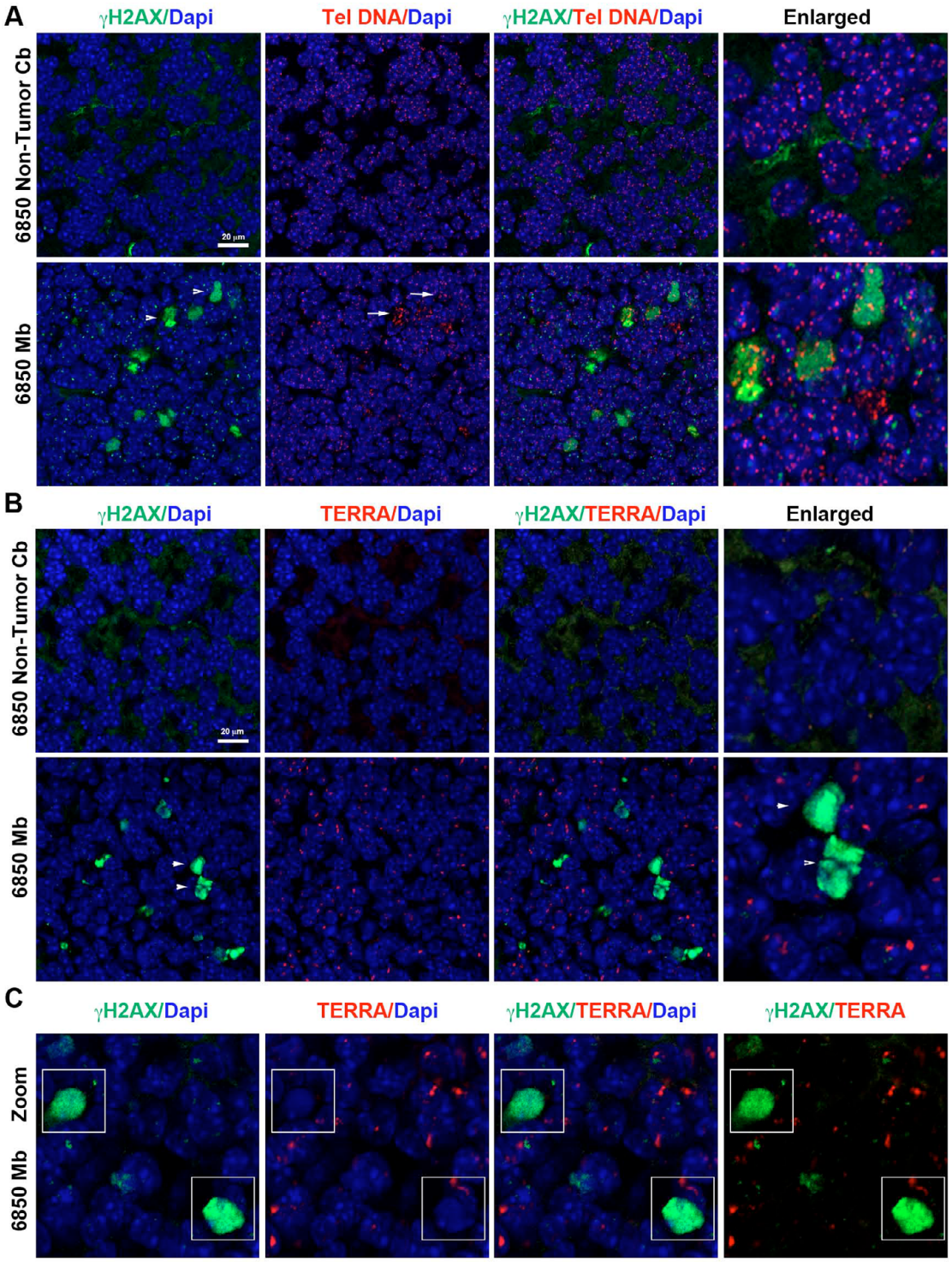

Fig. S6. Tumor-associated TERRA foci do not colocalize with γH2AX. (A) Confocal microscopy images of IF of γH2AX foci (green) combined with DNA FISH for telomere repeat DNA (TelDNA) (red) in non-tumor (non-T) or tumor sections (#6850). DAPI stain is in blue. Arrowheads indicate large γH2AX foci. Arrows indicate nuclei containing intense telomere DNA signals colocalization with large γH2AX foci. Enlarged image for merged image is shown in the right panel. Scale bar=20 μm. (B) Confocal microscopy images of IF of γH2AX foci (green) combined with RNA FISH for TERRA (red) in non-tumor or tumor sections of the cerebellum (#6850). Arrowheads indicate large γH2AX foci. Enlarged image for merged image is shown in the right panel. Scale bar=20 μm. (C) Zoomed images of IF of γH2AX foci (green) combined with RNA FISH for TERRA (red) in non-tumor or tumor sections of the cerebellum (#6850). Regions containing large γH2AX foci are shown in square.

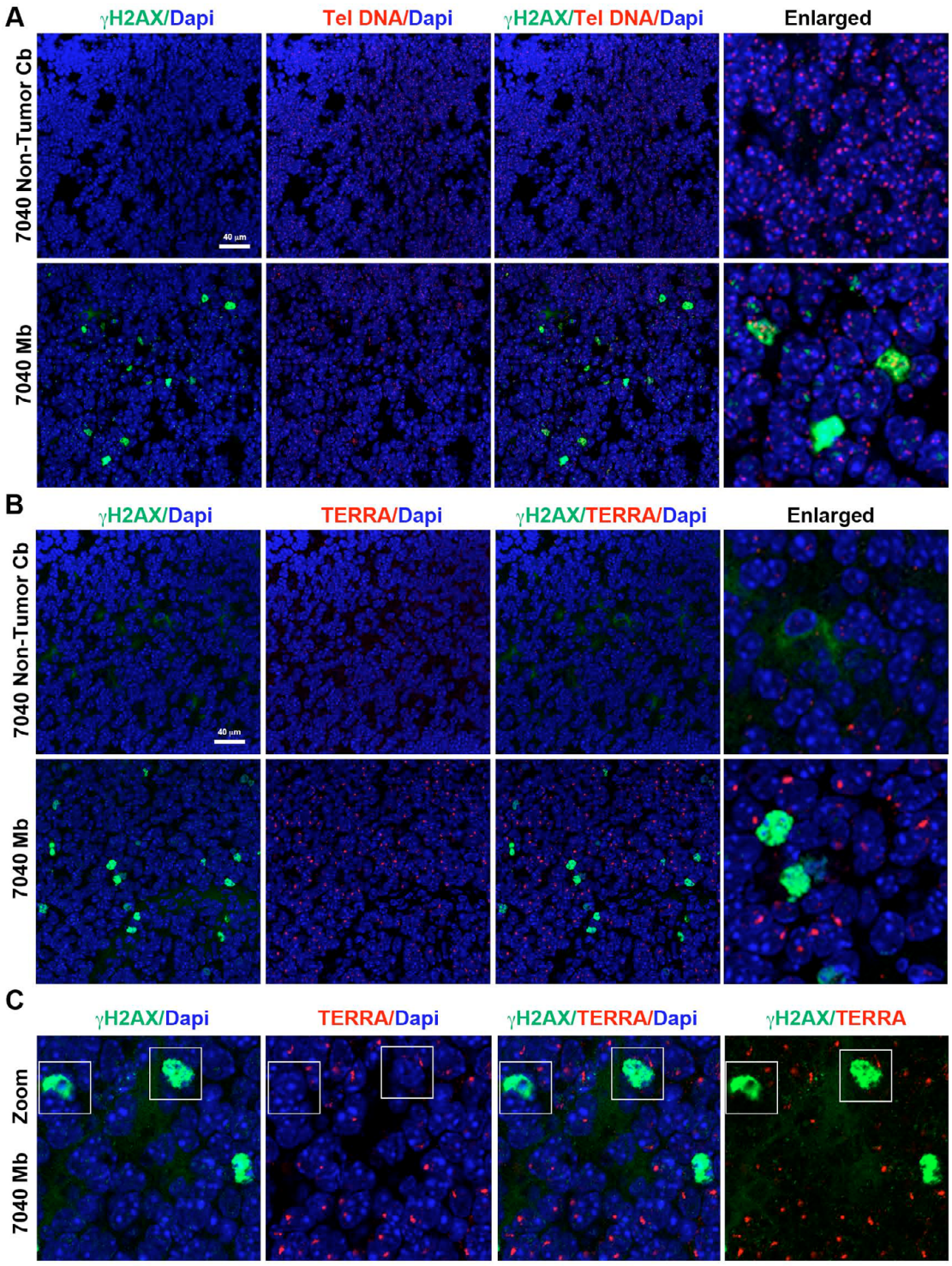

Fig. S7. Another example of tumor-associated TERRA foci do not colocalize with γH2AX. (A-C) Confocal microscopy was performed the same as that in Fig. S6, except that non-tumor or tumor sections of the cerebellum from #7040 were used in the assay.

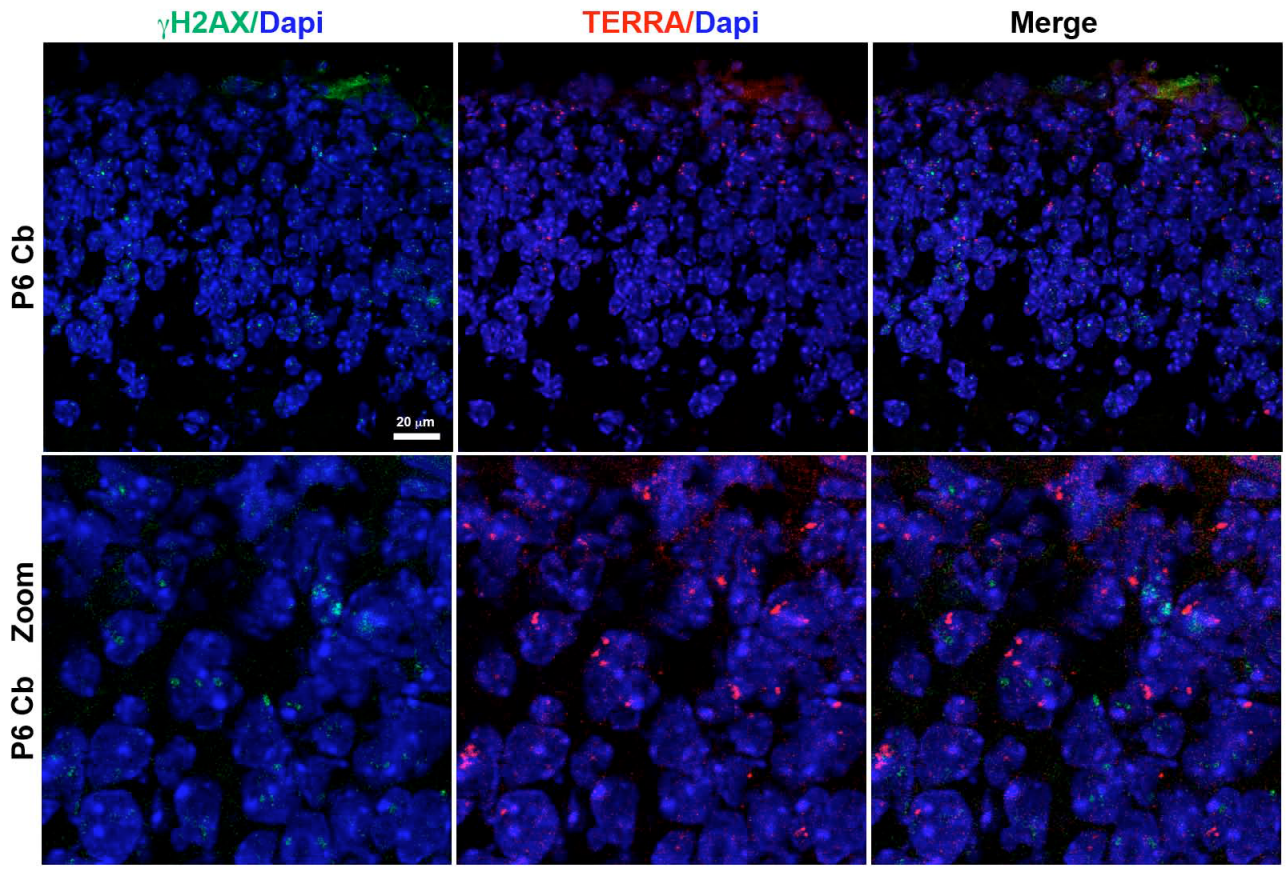

Fig. S8. TERRA foci do not colocalize with γH2AX in normal P6 cerebellum. Confocal microscopy images of IF of γH2AX foci (green) combined with RNA FISH for TERRA (red) in P6 normal cerebellum. DAPI stain is in blue. Zoomed image of the top panel is shown in the bottom panel. Note that no apparent large γH2AX foci was observed in P6 normal cerebellum. Scale bar=20 μm.

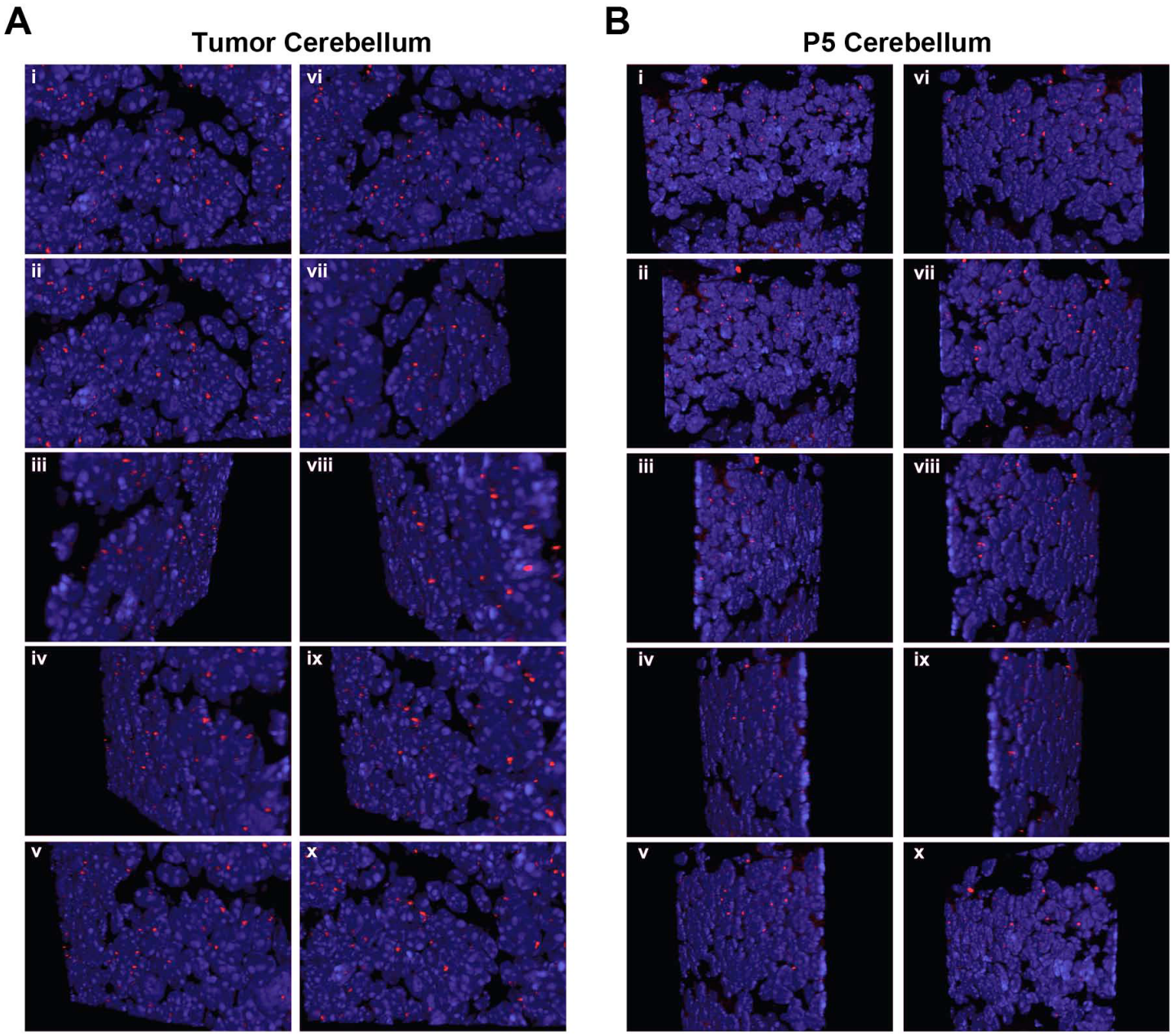

Fig. S9. 3D reconstruction of nuclear localization of TERRA RNA. (A) 3D confocal rendering of TERRA RNA FISH on tissues sections derived from mouse medulloblastoma (#7040). Different rotations around the XY plane are shown in each frame. TERRA signal is shown in red while nuclear stain by DAPI is in blue. (B) Same as in A, except in normal cerebellar tissue derived from stage P5 mouse.

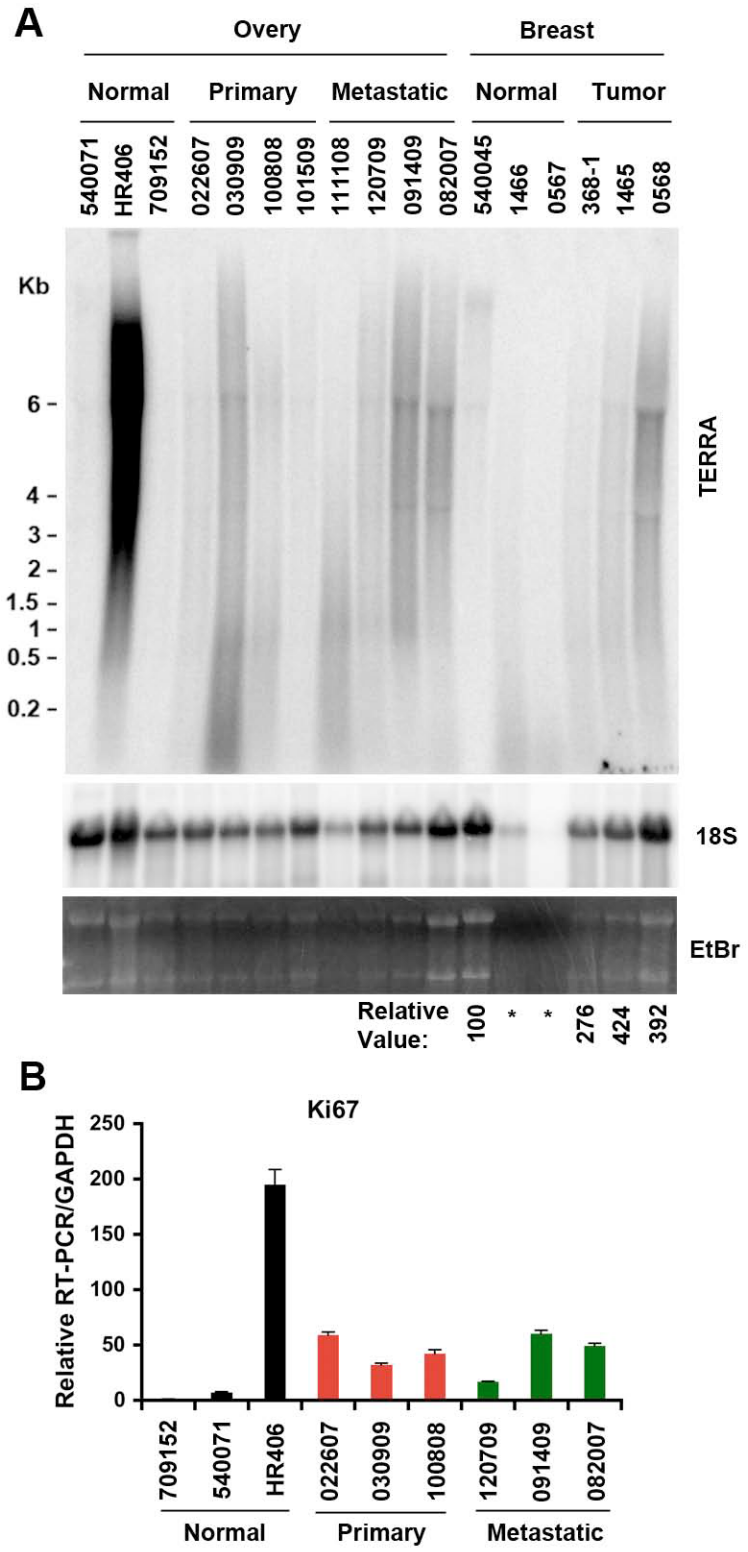

Fig. S10. TERRA expression in various human tumor tissues. (A) Northern blot analysis of TERRA RNA isolated from normal ovarian tissue, primary ovarian tumor, or metastatic ovarian cancer tissue, and normal breast tissue, or breast cancer tissue. Numbers at the bottom show the value of TERRA signals relative to 18S RNA signals in tumor versus normal breast tissues. (*) shows that the sample is not included in the analysis due to the degradation of 18S signal. Also note that normal ovary tissue (HR406) shows extremely high levels of TERRA expression. (B) qRT-PCR analysis of *Ki-67* expression in the indicated ovarian cancers and normal ovary tissue. ΔΔCT methods relative to normal ovary (R1234183, lot # A709152) and *Gapdh* were used to calculate relative RT-PCR between normal and tumor samples. Bar graph represents the average value from three independent PCR reactions (mean ± s.d.).

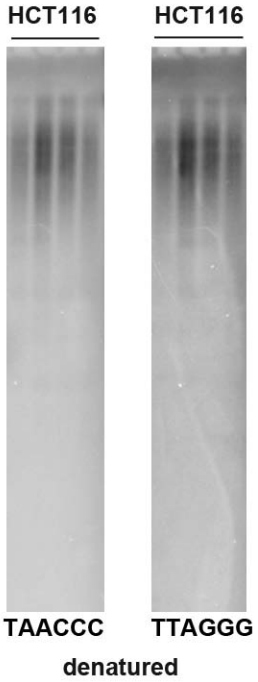

Fig. S11. A control experiment showing equal efficiency of hybridization for the G-rich and C-rich probes. Genomic DNA isolated from HCT116 cells were digested with *Alu*I/*Mbo*I and assayed by in gel hybridization under denaturing condition using either ^{32}P-labeled $(TAACCC)_4$ or ^{32}P-labeled $(TTAGGG)_4$ probe. Similar efficiency of hybridizations for denatured genomic DNA from both probes was observed.

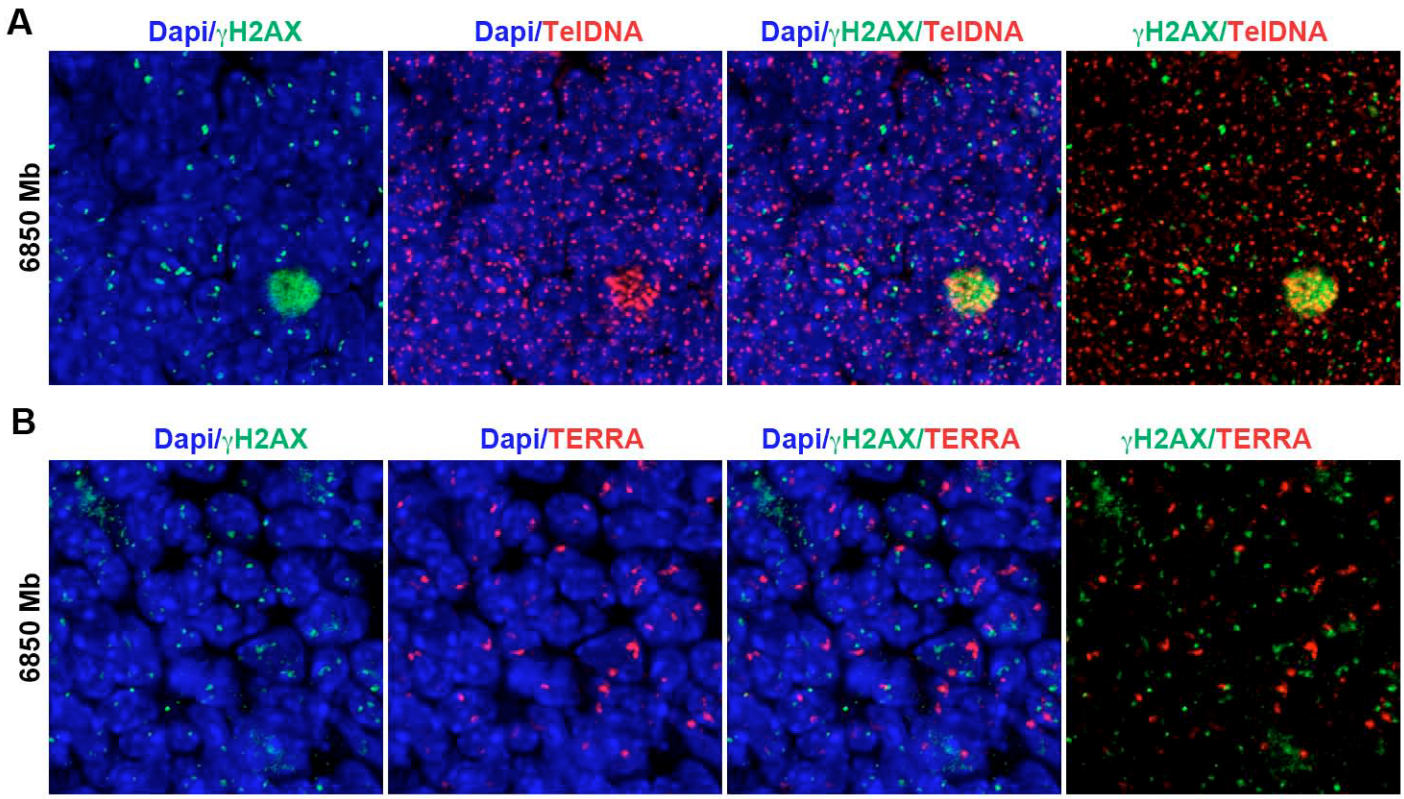

Fig. S12. Small γH2AX foci do not colocalize with TERF. Zoom image of small γH2AX foci and TelDNA (top panels) or TERRA (lower panels) from images described in Fig. S6.

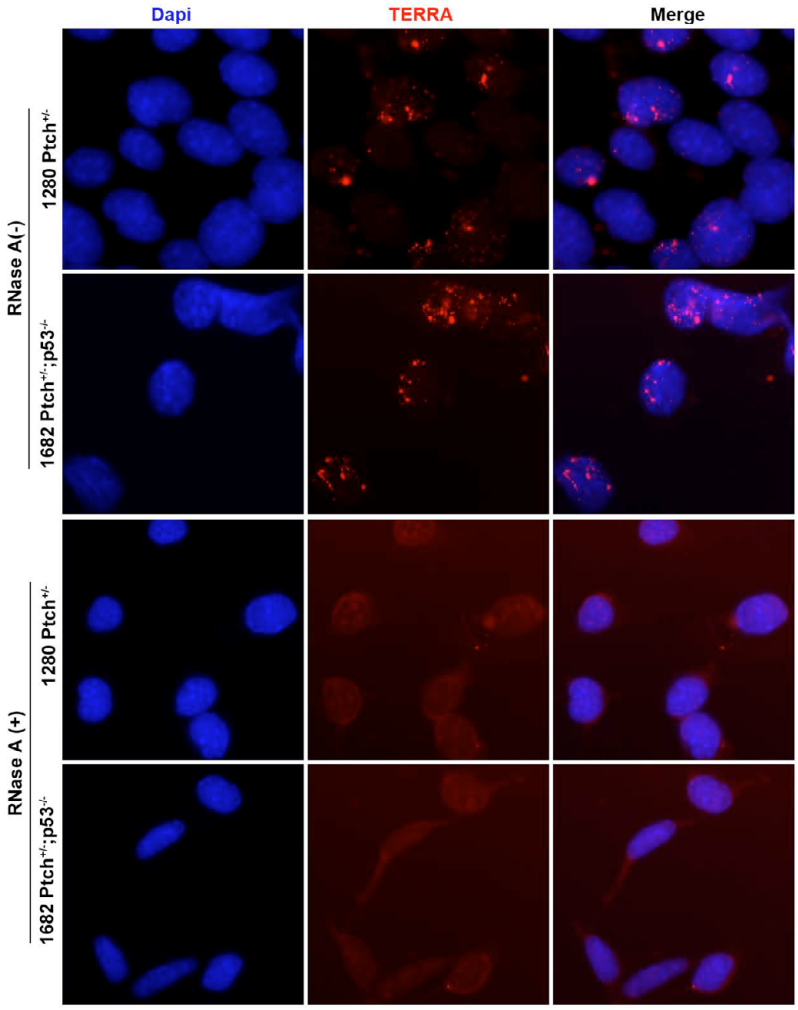

Fig. S13. RNA FISH of TERRA foci in mouse medulloblastoma cell lines. Two mouse medulloblastoma cell lines (1280, *Ptch1*$^{+/-}$; 1682, *Ptch1*$^{+/-}$ *p53*$^{-/-}$) were assayed using methods described for RNA-FISH used for tissue sections. TERF can be observed in both cell lines, but there is a higher percent of cells show TERF in 1682, which are p53 null and are derived from mouse strains with higher incidence of MB development in vivo.

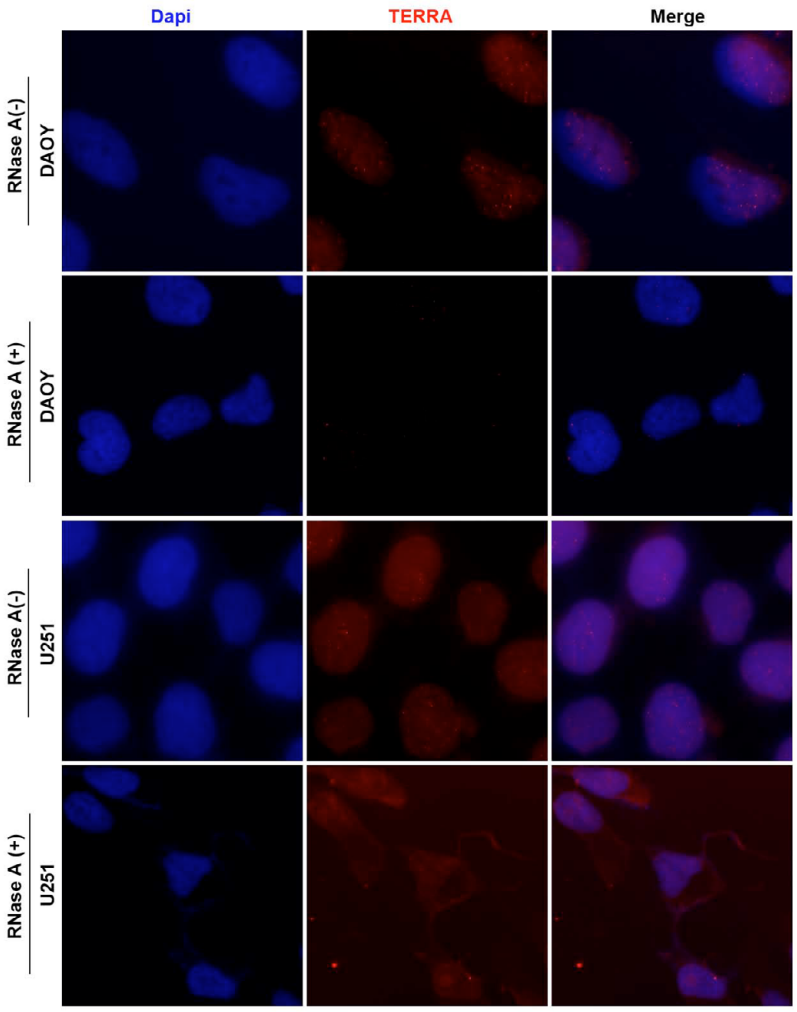

Fig. S14. RNA FISH of TERRA foci in human medulloblastoma and glioma cell lines. DAOY (human medulloblastoma cells) and U251 (human glioma cells) were subject to RNA-FISH using method described for mouse tissue FISH analysis. We observed smaller and fewer TERF in human medulloblastoma cell lines, relative to mouse medulloblastoma cell lines

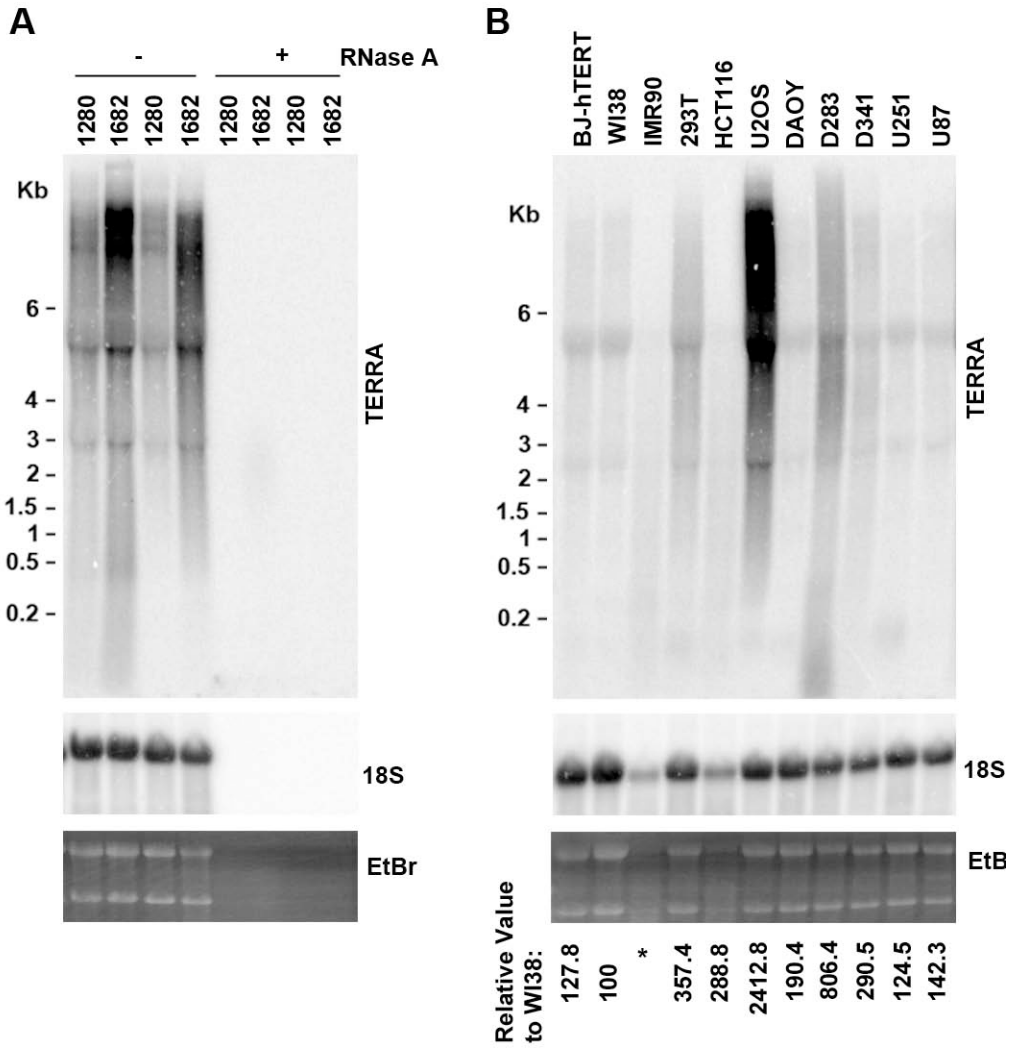

Fig. S15. Comparison of TERRA levels in multiple different cell lines. Northern blotting for TERRA levels in mouse medulloblastoma cells (A) and various human cell lines (B). Equal amount of total RNA (7.5 μg) isolated from each cell lines was used in the assay. We find no clear correlation of TERRA expression in immortalized vs. non-immortalized cell lines.

Table S1. List of primers used for quantitative RT-PCR

Transcript	Primer	Sequence (5′-3′)
m2q-TERRA	5′primer	TTTCCAGTGATGGCCGACTAG
m2q-TERRA	3′primer	CCCCGGAGCTCTTGACTCT
m5q-TERRA	5′primer	ATTAACAAGCACAAGAGGGTAGCA
m5q-TERRA	3′primer	CAACCATACCTGAAATGCCTAGATC
m11q-TERRA	5′primer	TGCCATTGGAACACAGCAA
m11q-TERRA	3′primer	CGTCTGCTGAGGTCCACAGA
mTeloCen-TERRA	5′primer	CCAAAGTTTCTGCAAGGCAAA
mTeloCen-TERRA	3′primer	CCCAATCTGTTGGTGGTCTTTT
M18q-TERRA	5′primer	CAGGCCAAAGAAGGGACAGA
M18q-TERRA	3′primer	GCTTCCTCACTGATCCACAGTACA
mGapdh	5′primer	CCATCAACGACCCCTTCATTGACC
mGapdh	3′primer	TGGTTCACACCCATCACAAACATG
mGli1(El-Zaatari et al., 2007)	5′primer	GCTGGAGGTCTGCGTGGTA
mGli1	3′primer	GGTGGAGTCATTGGATTGAACA
mMath1 (Zheng et al., 2000)	5′primer	CTGAACCACGCCTTCGACCAGCTG
mMath1	3′primer	TTGAAGGACGGGATAACGTTG
mMap2 (Armentano et al., 2006)	5′primer	AACATCAAATACCAGCCTAAGG
mMap2	3′primer	TGGCCTGTGACGGATGTTCT
h10q-TERRA	5′primer	CTGCACTTGAACCCTGCAATAC
h10q-TERRA	3′primer	GAATCCTGCGCACCGAGAT
hXqYq-TERRA	5′primer	CCCCTTGCCTTGGGAGAA
hXqYq-TERRA	3′primer	GAAAGCAAAAGCCCCTCTGA
h2q-TERRA	5′primer	GCCTTGCCTTGGGAGAATCT
h2q-TERRA	3′primer	AAAGCGGGAAACGAAAAGC
h13q-TERRA	5′primer	GCACTTGAACCCTGCAATACAG
h13q-TERRA	3′primer	CCTGCGCACCGAGATTCT
h15q-TERRA	5′primer	TGCAACCGGGAAAGATTTTATT